Single-Entity $Ti_3C_2T_x$ MXene Electro-oxidation

Pranati Nayak,[a] Minjun Yang, [a] Zhiwei Wang, [b] Xiuting Li, [b] Ruiyang Miao,[a]

Richard G. Compton*[a]

Department of Chemistry, Physical and Theoretical Chemistry Laboratory
Oxford University, South Parks Road, Oxford OX1 3QZ, United Kingdom
E-mail: richard.compton@chem.ox.ac.ukAddress here.

Institute for Advanced Study, Shenzhen University, Nanhai Avenue 3688,
Nanshan District, Shenzhen 518060, China.

ABSTRACT

We quantify the innate electro-oxidation behavior of a single $Ti_3C_2T_x$ MXene particle by Single-Entity Electrochemistry. MXene undergoes irreversible oxidation at potentials greater than 0.3 V (vs. SCE), with the extent of oxidation dependant on the applied potential. A close correlation is seen with ensembles of drop-cast particles with submonolayer coverage.

Keywords: Nanoimpact, MXenes, Cyclic voltammetry, Electrooxidation,

1. Introduction

Recently, "MXenes"- a new bourgeoning class of 2D layered material has been seen to be outperforming many others due to its particular physicochemical properties.[1] Akin to 2D graphene, MXenes are stacks of 2D early transition metal carbides, nitrides, and carbonitrides of general formula $M_{n+1}X_nT_x$, where M stands for transition metal atom, X stands for C and/or N, n = 1, 2, or 3, and T_x denotes various surface terminations (OH, O, and/or F groups). MXenes are typically produced by top-down wet-chemical roots by selectively etching out the A layers from ternary $M_{n+1}AX_n$ phases, where A is mainly a group IIIA or IVA (i.e., group 13 or 14) element. [2] The atoms inside a single layer are held by strong mixed metallic/covalent/ionic bonds, while the stacked layers are weakly bonded after the removal of the "A" layer from the parent MAX phase. The inner conductive carbon core, crammed by outer transition metal oxides/hydroxide-like surfaces and surface terminations in MXene (e.g. $Ti_3C_2T_x$ MXene, Fig. 1) enables a combination of metallic electron conductivity and hydrophilicity. [3]

Among the various members of the MXene family, the first reported titanium carbide ($Ti_3C_2T_x$) MXene possesses the highest reported electronic conductivity (> 10000 Scm^{-1}) and surface hydrophilicity suggesting its prospective use as electrode material in electrochemical applications, including energy storage, electronics, catalysis, and sensors, where it may outperform graphene.[4] Pristine graphene displays no inherent electrochemistry over a stable

and large window, although graphite oxide (GO) shows various electrochemical reductions originating from electroactive oxygen functionalities such as quinones.[5] In contrast with pristine graphene but similar to GO, $Ti_3C_2T_x$ possesses a conducting carbon core sandwiched by active Ti and surface terminations, which are prone to intrinsic redox reactions. The voltammetry of $Ti_3C_2T_x$ in an aqueous electrolyte shows a chemically irreversible oxidation signal on a first scan which rapidly diminishes in subsequent scans, indicating surface passivation and is inferred to arise from the formation of TiO_2.[6] Such oxides on $Ti_3C_2T_x$ MXene are reportedly beneficial for the claimed ultrasensitive detection of H_2O_2. Also, recent studies have suggested that partial anodic oxidation of $Ti_3C_2T_x$ MXene improves the electrochemical performance compared to pristine $Ti_3C_2T_x$ MXene electrodes.[7] On the other hand, some effort has been paid to preserve the surface chemistry of MXene from oxidation by depositing cobalt layered double hydroxide (Co-LDH) and Pt NPs over the surface, which is suggested to avoid the irreversible oxidation of $Ti_3C_2T_x$ MXene whilst simultaneously enhancing its stability in the anodic potential window.[8, 9]

Despite these preliminary investigations on the intrinsic oxidative nature of $Ti_3C_2T_x$ MXene and extensive research on its electrochemical applications as a catalyst, catalyst support, and co-catalyst,[4] a general literature search reveals a comparative lack of basic essential knowledge on the quantitative innate oxidation behavior or analysis of its origin. Taking note of the significant past wide research on $Ti_3C_2T_x$ MXene and the current vast interest to exploit MXene for a myriad of electrochemical applications, [4, 10, 11] we suggest that a quantitative analysis on the inherent oxidative properties is timely and prudent. Toward this objective, we report the first-ever study of single particles of $Ti_3C_2T_x$ MXene studied as a suspension in an aqueous solution via Single-Entity electrochemistry (SEE), a contemporary appealing electrochemical technique having the ability to quantify the response of individual microscopic entities via stochastic collision with the electrode surface (Nano-impact).[12] SEE has shown remarkable success on 0D nanoparticles,[13,14] 1D CNTs,[15] Nanorods,[16] and biological entities (e.g. bacteria, virus)[17,18] in the past. Of late its extension on 2D layered materials (graphene, transition metal dichalcogenides (TMDs)) [19,20] reveals extensive new mechanistic insights on their fundamental electrochemistry and novel applications. By implementing SEE, we explore the extent to which individual $Ti_3C_2T_x$ MXene particles can be electro-oxidized and find the material to be surprisingly resistant to electro-oxidation in aqueous electrolytes. The study is extended to define the implications for ensembles of $Ti_3C_2T_x$ MXene particles.

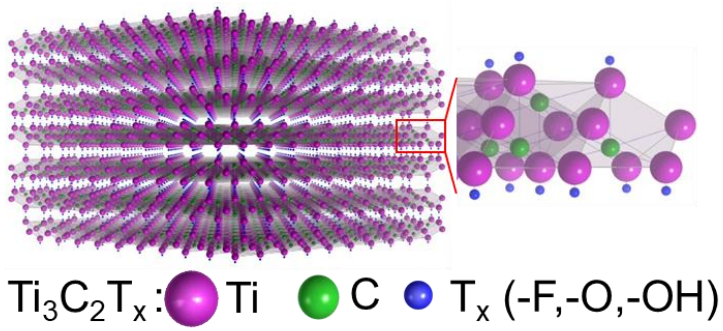

Fig.1 Schematic model showing the structure of $Ti_3C_2T_x$ MXene

2. Results and Discussion

$Ti_3C_2T_x$ MXene was prepared by wet-chemical etching of Ti_3AlC_2 MAX phase with HF according to the details described in Section 1, Supporting Information. After etching, the Ti_3AlC_2 bulk particles turn into accordion-like $Ti_3C_2T_x$ of average area (4.0 ± 0.2) μm^2 (from a total of 1182 particles of as-prepared MXene), as imaged via SEM and as shown in Fig. S1a-c, Section 1, Supporting Information. The as-prepared $Ti_3C_2T_x$ bulk particles are meta-stable in suspension for tens of seconds and seen to settle after a few minutes. However, for single-particle Nano-impact measurements, a stable suspension is essential to record information from the particle-electrode collision during its Brownian motion.[12] To achieve this, we separated the lighter $Ti_3C_2T_x$ particles via mild sonication followed by a sedimentation-based separation technique under centrifugal field and named Sample A and Sample B (details described in Section 2, Supporting Information, Fig. S2a-g). Controlled mild sonication effectively shatters MXene flakes and reduces their average lateral size, [21, 22] resulting in a stable dispersion of $Ti_3C_2T_x$ particles in samples A and B, which remains stable in suspension for over an hour. The concentrations of $Ti_3C_2T_x$ MXene particles in Sample A and Sample B were estimated by vacuum filtration (details in Section 3 Supporting Information) and correspond to 23 µg/ml and 103 µg/ml respectively. As illustrated in the FESEM images (Fig. 2a and Fig. S1d, e), a stacked 2D sheet-like morphology is observed for $Ti_3C_2T_x$ particles. Compared to as-prepared $Ti_3C_2T_x$ MXene bulk particles (4.0 ± 0.2) μm^2, the SEM particle areas for Sample A and B are smaller (2.2 ± 0.1 μm^2 and 3.5 ± 0.4 μm^2) as evident from the distribution plot of projection areas for both the samples (from a total of 464 particles from Sample A-Fig. 2b and 223 particles from Sample B-Fig. S1f).

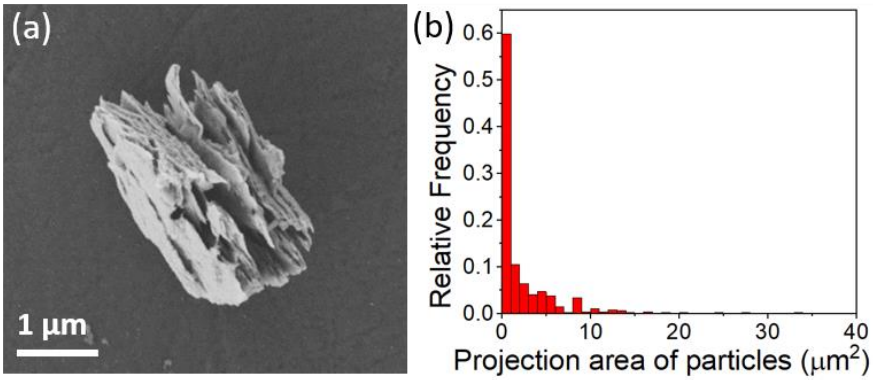

Fig. 2 *(a) Field emission scanning electron microscopy (FESEM) image of $Ti_3C_2T_X$ MXene from Sample A, (b) plot of relative frequency vs projection area from the FESEM images of a total of 464 particles.*

This size reduction resulting from mild ultrasonication possibly enhances the stability of $Ti_3C_2T_x$ MXene particles in the dispersion.

To explore the oxidation of $Ti_3C_2T_x$ particles at a single particle level, nano-impact measurements were carried out by inserting a clean carbon fiber micro-wire electrode (length ca. 1 mm and diameter ca. 7 µm) into a dispersion containing Sample A (23 µg/ml) in 0.1 M H_2SO_4 (details in Section 4, Supporting Information). Figure S3, Supporting Information shows an image captured by optical microscopy showing the suspended MXene particles in solution where they were observed to undergo Brownian motion. Chronoamperograms were immediately recorded at a series of applied potentials from 0 V to 1.3 V vs. saturated calomel electrode (SCE). As evident from Fig. 3a, several current spikes appear in the amperogram ascribed to electron transfer to the potentiostated electrode due to possible oxidation during the stochastic collision of single $Ti_3C_2T_x$ particles with the electrode. In a typical spike (inset of Fig. 3a), the sharp current step-up signals the arrival of the single entity at the electrode surface, and the duration of the current step reflects its residence time followed by a sharp step-off, indicative of departure of the entity from the electrode surface. The average oxidative charge was calculated by integrating the area of each spike and a large number, "n", spikes were considered from several chronoamperograms at a particular applied potential. The plot of average impact charge Q_{avg} vs. applied potential (Fig. 3b) reveals an onset oxidative potential around 0.3 V, whilst a notable increase of Q_{avg} is observed with a progressive increase of applied potential. The values of Q_{avg} at potentials more positive than 1V tend towards a plateau, suggestive of maximum oxidation of $Ti_3C_2T_x$ particles at a high applied potential. The error bar was derived from the equation $SD/(n)^{1/2}$, where SD is the

standard deviation and "n" is the number of spikes. Fig. 3c shows the distribution of charge of spikes at the highest potential, reflecting the range of size of $Ti_3C_2T_x$ particles present. The average charge was determined to be (1.7 ± 0.3) nC from a total of 81 spikes. The plot of ln(Q) against ln(t) (Fig. 3d) depicts a reasonable linear dependence, suggestive of an increase in oxidation with impact time. Very similar oxidative features were observed for Sample B (Fig. S4a, b, Supporting Information) with an onset oxidative potential ~0.3 V and plateau depicting maximum oxidation at potential more positive than 1V. However, a slightly lower average charge (1.1 ± 0.2 nC, Fig. S4c) was obtained at the highest potential compared to Sample A. Although scattered, a reasonable linear dependence is observed for the plot of ln(Q) against ln(t) (Fig. S4d). The chronoamperograms recorded at different applied potential are shown in Fig. S5, Supporting Information.

Having evidenced the electro-oxidation of single $Ti_3C_2T_x$ particles through SEE measurements, the study was extended to an ensemble of $Ti_3C_2T_x$ particles by drop-casting particles onto a conventional glassy carbon (GC) macro electrode. About 4 µl aliquot of $Ti_3C_2T_x$ particles (Sample A) suspension was drop-casted over GCE and air-dried. Cyclic voltammetry was conducted on the $Ti_3C_2T_x$ particles modified GCE in 0.1 M H_2SO_4. The voltammogram for Sample A particles shows an irreversible oxidation peak in the anodic potential window with peak potential at ca. ~0.7 V (Fig. 4a). No oxidative feature is observed in the second scan, suggestive of complete passivation of $Ti_3C_2T_x$ particles in the first scan. A very similar observation was seen for as-prepared $Ti_3C_2T_x$ particles and Sample B, as shown in Fig. S6a, d, Section 5, Supporting Information. Analogous experiments were carried out for different aliquots of dispersion drop-cast over GCE. A clear increase of oxidation peak current is seen in the voltammogram (Fig. S6b, e, and Fig. S7), validating the expected increase in oxidation with an increase in material loading (Fig. 4b and Fig. S6c, f). Along with the oxidation peak, a small reduction peak appeared in the CVs (Fig. 4a, Fig. S6a, b, d, e) for MXene modified GCE, which also appears for bare GCE. This is likely due to the oxygen reduction reaction (ORR). The possible mechanism of oxidation is speculated to be the following reaction:[6]

$$Ti_3C_2T_x + 8H_2O \longrightarrow 3TiO_2 + 2CO + 16H^+ + (16\text{-}x)\, e^- + xT^- \quad \text{(1)}$$

However, the possibility on the formation of CO_2 as an oxidation product cannot be excluded. For $Ti_3C_2T_x$ MXene, the T_x number per formula unit is found to be ~2 from recent studies. [23] Based on this, the average % of total Ti converted into

TiO_2 is calculated to be ca. 2.3 % for $Ti_3C_2T_x$ particles in Sample A, and less for Sample B (1.1 %) and as-prepared $Ti_3C_2T_x$ particles (0.9 %). The average oxidation calculated per single particle from the average impact charge (Fig. 3c) is 2 % for Sample A and 0.7 % for Sample B respectively. The apparent decrease in oxidation for Sample B and the as-prepared $Ti_3C_2T_x$ particles compared to Sample A can be related to their comparatively larger size (evident from the SEM projection areas), and hence smaller surface area to volume ratio. The size-dependent electro-oxidative features correlate with the reported size-

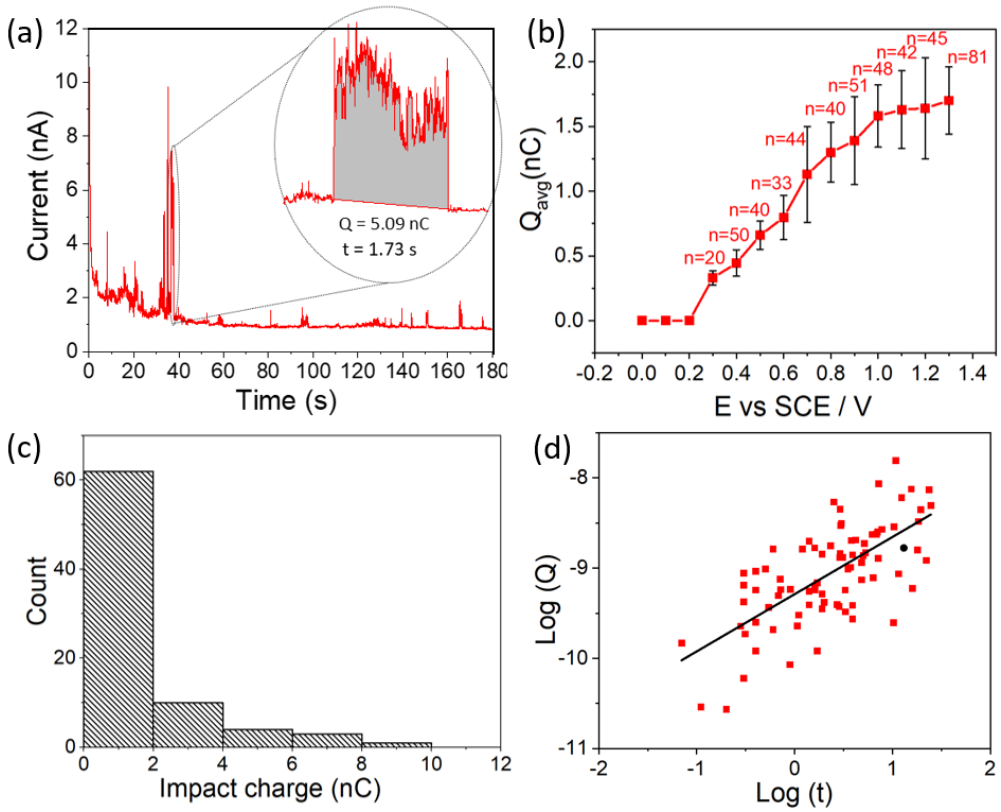

Fig.3 *(a) Chronoamperogram recorded at a carbon fiber microwire electrode in a 23 µg/ml $Ti_3C_2T_x$ MXene suspension in 0.1 M H_2SO_4 at 1.3 V applied potential vs. SCE, (b) Plot of Q_{avg} as a function of applied potential E; the error bars are derived from $SD/(n)^{1/2}$, where SD is the standard deviation and n is the number of the spikes. (c) Distribution of charge from oxidation of single particles spikes by analysis of 81 current spikes at 1.3 V applied potential vs. SCE, (d) the linear fitting (black line) of the natural logarithm of individual spike charge (Q) vs. logarithm of time. The black dot indicates the logarithm of average charge per particle vs logarithm of time from the drop-cast.*

dependent chemical oxidation of MXene at the exposed sites on the sheet edge or the basal plane, that originate during the harsh chemical etching of $Ti_3C_2T_x$ MXene.[24, 25] Apart from $Ti_3C_2T_x$ MXene, the size and edge-plane dependant electrochemistry is also widely validated for other layered materials ca. graphite,[26] graphenes,[27] black phosphorous,[28] and transition metal chalcogenides,[29] where changed electrochemical

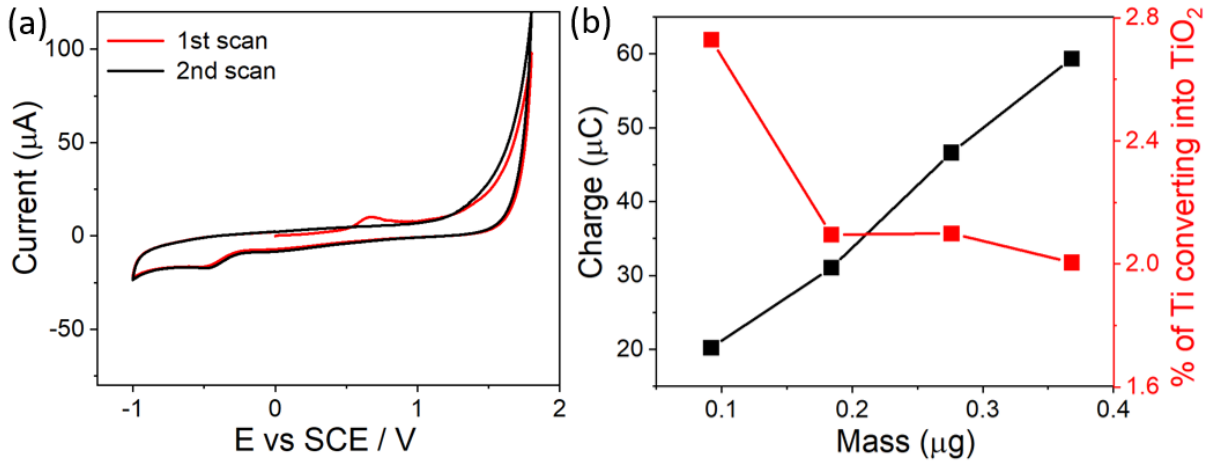

Fig. 4 (a) Voltammogram at GCE modified with $Ti_3C_2T_x$ MXene (Sample A) for two repeated scans in 0.1 M H_2SO_4. The plot of charge and % of Ti converting into TiO_2 vs mass of particles drop cast over GCE. Reference electrode: SCE; Scan rate: 100 mV/s.

reactions with size reduction likely reflect surface area to volume ratios. In addition, the oxidation product (TiO_2) is same as that produced by thermal oxidation of MXene in controlled air atmosphere, which is reportedly beneficial for several electrochemical applications.[30,31] The average charge per particle from the voltammetry at the drop-cast electrode was calculated from the average number of particles in the drop-cast and the average projection area assuming the particles are cubic (detailed calculation in Section 6, Supporting Information, Fig. S8). The plot of log(Q) vs log(t) calculated from the average oxidation charge per particle (Q) and average oxidation time (t) from drop-casted particles is superimposed (black dot in Fig. 3d) over the scattered log(Q) vs log(t) plot from impact measurements. A careful perusal of the plot suggests a fair correlation between the two datasets. Analogous calculations are done for Sample B particles and log(Q) vs log(t) is plotted over the impact plot (red dot in Fig. S4d, Supporting Information), which is found consistent with the $Ti_3C_2T_x$ MXene particles from Sample A. The correlation validates SEE measurement as a potential tool for understanding MXene electrochemistry at a single-particle scale.

To further validate the above we characterized $Ti_3C_2T_x$ MXene ensembles by X-ray photoelectron spectroscopy (XPS) and Raman spectroscopy before and after electro-oxidation. The experimental details of XPS are discussed in Section 1, Supporting Information. Fig. S9a depicts the CV of the as-prepared $Ti_3C_2T_x$ MXene ensembles, showing the electro-oxidation at positive potentials. Fig. S9b depicts the deconvoluted high-resolution Ti 2p spectra revealing different valence/charged states of Ti tentatively assigned to Ti-C, Ti-O, Ti-O_2, Ti-$O_{2-x}F_x$ and C-Ti-O/F_x.[23] As seen, the deconvoluted spectrum contains many overlapping peaks along with

a qualitative increase in the ratio of oxygen to Ti consistent with Ti oxidation. Overall some net loss of Ti from the surface was seen (Fig. S9c) and speculated to be due to the likely formation of soluble Ti species during the multi-step formation of TiO_2 from Ti and leading to leaching from the surface during electro-oxidation. Fig. S10 shows the comparison of Raman spectra for the as-prepared $Ti_3C_2T_x$ MXene and oxidised $Ti_3C_2T_x$ MXene. It is evident that the intensity of the peaks corresponding to $Ti_3C_2T_x$ MXene (at 214 and 705 cm^{-1}) decrease after electrochemical oxidation. This can be due to the presence of defects and holes after oxidation weakening the out-of-plane vibration.[7] The peaks in the range of 1100 to 1700 cm^{-1} could be attributed to C-C bonds from amorphous carbon produced by the oxidation of $Ti_3C_2T_x$. This also supports the XPS results on the formation of soluble Ti species in acidic electrolyte leaving amorphous carbon in the MXene surface.

3. Conclusions

To conclude, the intrinsic oxidation of individual $Ti_3C_2T_x$ MXene particles is studied both by single entity electrochemistry and conventional drop-cast measurements in this work. Impact measurements revealed that $Ti_3C_2T_x$ MXene undergoes irreversible oxidation in the anodic potential window (> 0.3 V), with a dependence of the extent of oxidation on the applied electrode potential. At the highest applied potential (ca. 1.3 V), oxidation up to ca. 2 % of total Ti (Sample A) is observed, which further declines to 0.7 % for Sample B, attributed to a change in the surface area to volume ratio. These charges transferred showed a close correlation with that seen in the voltammetry of drop-cast particles (2.3 % for Sample A and 1.1 % for Sample B) at least for up to sub-mono layers of particles. This work provides the first-ever study on quantitative innate electro-oxidation behavior of $Ti_3C_2T_x$ MXene down to a single particle with a fair resemblance to a dispersed ensemble of particles.

Acknowledgments

PN acknowledges the Royal Society, UK for support through a Newton-Bhaba International Fellowship (Grant number- NIF\R1\180784). Z. Wang and X. Li acknowledge the grants from the Regional Joint Fund of Guangdong Province (2019A1515111054) and the National Natural Science Foundation of China (22004085).

Conflicts of interest

There is no conflict to declare.

References

[1] M. Naguib, M. Kurtoglu, V. Presser, J. Lu, J. Niu, M. Heon, L. Hultman, Y. Gogotsi, M. W. Barsoum, Two-Dimensional Nanocrystals Produced by Exfoliation of Ti_3AlC_2, Adv. Mater. 23 (2011) 4248-4253.

[2] M. Naguib, V. N Mochalin, M. W. Barsoum, Y. Gogotsi, 25th Anniversary Article: MXenes: A New Family of Two-Dimensional Materials, Adv. Mater. 26 (2014) 992-1004.

[3] M. Naguib, O. Mashtalir, J. Carle, V. Presser, Jun Lu, Lars Hultman, Y. Gogotsi, Michel W. Barsoum, Two-Dimensional Transition Metal Carbides, ACS Nano 6 (2012) 1322-1331.

[4] A. V. Mohammadi, J. Rosen, Y. Gogotsi, The world of two-dimensional carbides and nitrides (MXenes), Science 372 (2021) 1165-1179.

[5] H. S. Toh, A. Ambrosi, C. K.Chua, M. Pumera, Graphene Oxides Exhibit Limited Cathodic Potential Window Due to Their Inherent Electroactivity, J. Phys. Chem. C 115 (2011) 17647-17650.

[6] L. Lorencova, T. Bertok, E. Dosekova, A. Holazova, D. Paprckova, A. Vikartovska, V. Sasinkova, J. Filip, P. Kasak, M. Jerigova, D. Velic, K.A. Mahmoud, J. Tkac, Electrochemical performance of $Ti_3C_2T_x$ MXene in aqueous media: towards ultrasensitive H_2O_2 sensing, Acta Electrochim. 235 (2017) 471-479.

[7] J. Tang, T. S. Mathis, N. Kurra, A. Sarycheva, X. Xiao, M. N. Hedhili, Q. Jiang, H. N. Alshareef, B. Xu, F. Pan, Y. Gogotsi, Tuning the Electrochemical Performance of Titanium Carbide MXene by Controllable In Situ Anodic Oxidation, Angew. Chem., Int. Ed. 58 (2019) 17849-17855.

[8] M. Benchakar, T. Bilyk, C. Garnero, L. Loupias, C. Morais, J. Pacaud, C. Cana, P. Chartier, S. Morisset, N. Guignard, V. Mauchamp, S. Celerier, A. Habrioux, MXene Supported Cobalt Layered Double Hydroxide Nanocrystals: Facile Synthesis Route for a Synergistic Oxygen Evolution Reaction Electrocatalyst, Adv. Mater. Interfaces, 6 (2019) 1901328.

[9] L. Lorencova, T. Bertok, J. Filip, M. Jerigova, D. Velic, P. Kasak, K.A. Mahmoud, J. Tkac, Highly stable $Ti_3C_2T_x$(MXene)/Pt nanoparticles-modified glassy carbon electrode for $H_2O_2$and small molecules sensing applications, Sens. Actuators B 263 (2018) 360-368.

[10] J. Zhao, L. Zhang, X.-Y. Xie, X. Li, Y. M, Q. Liu, W.-H. Fang, X. Shi, G. Cui and X. Sun. $Ti_3C_2T_x$ (T = F, OH) MXene nanosheets: conductive 2D catalysts for ambient electro hydrogenation of N_2 to NH_3. J. Mater. Chem. A, 6 (2018) 24031-24035.

[11] W. Kong, F. (Frank) Gong, Q. Zhou, G. Yu, L. Ji, X. Sun, A. M. Asiri, T. Wang, Y. Luoe and Y. Xub, MnO_2-$Ti_3C_2T_x$ MXene nanohybrid: an efficient and durable electrocatalyst toward artificial N_2 fixation to NH_3 under ambient conditions. J. Mater. Chem. A, 7 (2019) 18823-18827.

[12] S. V. Sokolov, S. Eloul, E. Ka¨telho¨n, C. Batchelor-McAuley, R. G. Compton, Electrode-particle impacts: a user's guide, Phys. Chem. Chem. Phys. 19 (2017) 28-43.
[13] Y. G. Zhou, N.V. Rees, R. G. Compton, The Electrochemical Detection and Characterization of Silver Nanoparticles in Aqueous Solution, Angew. Chem. Int. Ed. 50 (2011) 4219-4221.
[14] E. J. E. Stuart, K. Tschulik, C. B. McAuley, R. G. Compton, Electrochemical Observation of Single Collision Events: Fullerene Nanoparticles, ACS Nano 8 (2014) 7648-7654.
[15] X. Li, C. B. McAuley, L. Shao, S. V. Sokolov, N. P. Young, R. G. Compton, Quantifying Single-Carbon Nanotube-Electrode Contact via the Nanoimpact Method J. Phys. Chem. Lett. 8 (2017) 507-511.
[16] B. J. Plowman, N. P. Young, C. Batchelor-McAuley, R. G. Compton, Nanorod Aspect Ratios Determined by the Nano-Impact Technique, Angew. Chem. Int. Ed. 55 (2016) 7002-7005.
[17] R. A. S. Couto, L. Chen, S. Kuss, R. G. Compton, Detection of Escherichia coli bacteria by impact electrochemistry Analyst 143 (2018) 4840-4844.
[18] L. Sepunaru, B. J. Plowman, S. V. Sokolov, N. P. Young, R. G. Compton, Rapid electrochemical detection of single influenza viruses tagged with silver nanoparticles, Chem. Sci.**7** (2016) 3892-3899.
[19] R. Miao, L. Chen, L. Shao, B. Zhang, R. G. Compton, Electron Transfer to Decorated Graphene Oxide Particles, Angew. Chem. Int. Ed. 58 (2019) 12549-12552.
[20] C. S. Lim, S. M. Tan, Z. Sofer, M. Pumera, Impact Electrochemistry of Layered Transition Metal Dichalcogenides, ACS Nano 9 (2015) 8474-8483.
[21] M. Malaki, A. Maleki, R. S. Varma, MXenes and ultrasonication, J. Mater. Chem. A, **7** (2019) 10843.
[22] K. Maleski, C. E. Ren, M. Q. Zhao, B. Anasori, Y. Gogotsi, Size-Dependent Physical and Electrochemical Properties of Two-Dimensional MXene Flakes. ACS Appl. Mater. Interfaces 10 (2018) 24491-24498.
[23] J. Halim, K. M. Cook, M. Naguib, P. Eklund, Y. Gogotsi, J. Rosen, M. W. Barsoum, X-ray photoelectron spectroscopy of select multi-layered transition metal carbides (MXenes), Appl. Surf. Sci. 362 (2016) 406-417.
[24] C. J. Zhang, S. Pinilla, N. McEvoy, C. P. Cullen, B. Anasori, E. Long, S. H. Park, A. S. Ascaso, A. Shmeliov, D. Krishnan, C. Morant, X. Liu, G. S. Duesberg, Y. Gogotsi, Valeria Nicolosi Oxidation Stability of Colloidal Two-Dimensional Titanium Carbides (MXenes), Chem. Mater. 29 (2017) 4848-4856.
[25] A. Iqbal, J. Hong, T. Y. Ko, C. M. Koo, Improving oxidation stability of 2D MXenes: synthesis, storage media, and conditions Nano Converge 8 (2021) 1-22
[26] T. J. Davies, M. E. Hyde, R. G. Compton, Nanotrench Arrays Reveal Insight into Graphite Electrochemistry, Angew. Chem. Int. Ed. 44 (2005) 5121-5126.
[27] B. Zhang, L. Fan, H. Zhong, Y. Liu, S. Chen, Graphene Nanoelectrodes: Fabrication and Size-Dependent Electrochemistry, J. Am. Chem. Soc. 135 (2013) 10073-10080.
[28] J. Wang, D. Liu, H. Huang, N. Yang, B. Yu, M. Wen, X. Wang, P. K. Chu, X. F. Yu, Edge-Rich Black Phosphorus for Photocatalytic Nitrogen Fixation. Angew. Chem. Int. Ed. 57 (2018) 2600-2604.
[29] T. F. Jaramillo, K. P. Jørgensen, J. Bonde, J. H. Nielsen, S. Horch, I. Chorkendorff. Identification of Active Edge Sites for Electrochemical H_2 Evolution from MoS_2 Nanocatalysts Science 317 (2007) 100-104.

[30] M. Naguib, O. Mashtalir, M. R. Lukatskaya, B. Dyatkin, C. Zhang, V. Presser, Y. Gogotsi, M. W. Barsoum, One-step synthesis of nanocrystalline transition metal oxides on thin sheets of disordered graphitic carbon by oxidation of MXenes. Chem. Commun. 50 (2014) 7420-7423.

[31] H. Ghassemi, W. Harlow, O. Mashtalir, M. Beidaghi, M. R. Lukatskaya, Y. Gogotsi, M. L. Taheri, In situ environmental transmission electron microscopy study of oxidation of two-dimensional Ti_3C_2 and formation of carbon-supported TiO_2. J. Mater. Chem. A 2 (2014) 14339.

[32] C. B. McAuley, J. Ellison, K. Tschulik, P. L. Hurst, R. Boldt, R. G. Compton, Get More Out of Your Data: A New Approach to Agglomeration and Aggregation Studies Using Nanoparticle Impact Experiments, Analyst 140 (2015) 5048-5054.

[33] J. Ellison, K. Tschulik, E. J. Stuart, K. Jurkschat, D.Omanovic, M. Uhle-mann, A. Crossley, R. G. Compton, In situ nanoparticle sizing with zeptomole Sensitivity. Chemistry Open 2 (2013) 69-75.